Physica B 609 (2021) 412893

Contents lists available at ScienceDirect

Physica B: Physics of Condensed Matter

journal homepage: www.elsevier.com/locate/physb

Electrical magnetotransport properties of chlorinated CVD graphene

F. Mesquita [a], G. Copetti [a], M.A. Tumelero [a], M.A. Gusmão [a], C. Radtke [b], P. Pureur [a,*]

[a] Instituto de Física, Universidade Federal do Rio Grande do Sul, 91501-970 Porto Alegre, RS, Brazil
[b] Instituto de Química, Universidade Federal do Rio Grande do Sul, 91501-970 Porto Alegre, RS, Brazil

ARTICLE INFO

Keywords:
Graphene CVD
Magnetoresistance
Weak localization
Hall effect

ABSTRACT

We report on electrical resistivity, magnetoresistance, and Hall-effect experiments in single-layer CVD graphene submitted to photochlorination. The resistivity and the ordinary Hall effect reveal a strong hole doping due to Cl adsorption. Intrinsic disorder of the as-grown system as well as that produced in the chlorination process lead to weak-localization effects, observed in the low-temperature magnetoresistance. The theoretically predicted regime where intervalley scattering fully restores the usual negative magnetoresistance is observed in a freshly chlorinated sample. Also observed are time-dependent effects in the electrical transport properties of the functionalized CVD-graphene samples due to a progressive loss of adsorbed Cl.

1. Introduction

Nowadays, graphene is probably the most studied two-dimensional atomic lattice [1]. Single-layer graphene has unique electronic, mechanical, thermal, optical, and other singular properties that make this material extremely attractive for fundamental studies as well as for several promising technical applications [1,2]. However, impurities, vacancies, adsorbed atoms, contact with the substrate, and other deviations from perfect ordering or the strict single-layer scenario may have strong influence on graphene's physical properties, especially the electronic ones [3]. An example is the recent surprising discovery of superconductivity in twisted double-layer graphene [4].

Although exfoliation from graphite is a largely used technique for obtaining graphene with superior properties, chemical vapor deposition (CVD) becomes a current method to produce continuous layers of good-quality graphene [5]. Since this technique depends on several parameters and conditions, samples usually do not show the striking electronic behavior of suspended exfoliated graphene [3,5]. However, CVD graphene may be grown into large surfaces, which is a necessary condition for making possible several envisaged applications of this material [2]. Thus, a detailed study of samples prepared by the CVD technique is of great interest.

One of the essential questions related to CVD graphene concerns the possibility of doping, either by substitution [6,7] or by functionalization [8], to control and enhance its electrical conductivity. Interesting attempts have been made to produce extended and stable modifications in the carrier density of CVD graphene by adsorption of halogens [9,10]. In particular, adsorbed chlorine atoms, which are highly electronegative, capture electrons from the graphene π bands, resulting in *p*-type doping.

In this communication, we report on electrical resistivity, magnetoresistance, and Hall-effect experiments in CVD graphene submitted to photochlorination. Focus is given to doping effects due to Cl adsorption, as well as to disorder related to the chlorination process, which is found to significantly influence the electron-scattering mechanisms in the functionalized material. In particular, disorder leads to the observation of weak-localization contributions to the low-temperature magnetoresistance. The limit where intervalley scattering fully restores the usual negative magnetoresistance is observed in a freshly chlorinated sample. Also observed are time-dependent effects on the Hall coefficient of the functionalized samples due to progressive loss of adsorbed Cl. To single out the effects of Cl incorporation, a pristine CVD graphene sample is also studied.

2. Experimental details

Millimeter-size samples were cut from large commercial pieces of CVD graphene furnished by Graphene Supermarket@, which consist of single-layer graphene grown on polycrystalline Cu foils, and transferred onto SiO_2 films (285 nm thick) covering a Si wafer. Some of these samples were submitted to a photochlorination process. The method was developed by Li et al. [11], and consists of exposing the samples to a Cl_2 flow under UV light, which was provided by a xenon–mercury lamp in our apparatus [10]. Shortly after chlorination, the Cl/C ratio reached values in the range of 0.1–1 [10,11]. But it has been clearly shown [10] that desorption of Cl adatoms occurs continuously under air exposure. One of the pristine samples (labeled as CVDg), with 3×6 mm^2 size, and two of the chlorinated samples, with 6×6 mm^2

* Corresponding author.
E-mail address: ppureur@if.ufrgs.br (P. Pureur).

https://doi.org/10.1016/j.physb.2021.412893
Received 17 October 2020; Received in revised form 26 January 2021; Accepted 5 February 2021
Available online 12 February 2021

size, were selected for electrical transport measurements. Six gold pads were deposited by low-energy sputtering on the graphene sheets to provide electrical contacts. These pads were appropriately placed to perform four-point longitudinal-resistivity and five-point Hall-voltage measurements [12], as shown schematically in the inset of Fig. 1. Wires were attached to the pads using silver paint.

To check for time-dependent effects due to Cl desorption, measurements on one of the chlorinated samples (labeled as CVDg-Cl) were made twice. In a first set of experiments, resistivity, magnetoresistance, and Hall-effect were measured after one day of exposure to the air atmosphere following the chlorination process. These measurements were then repeated nine days after Cl incorporation. The two states of the CVDg-Cl sample are named CVDg-Cl(1 day) and CVDg-Cl(9 days). The second chlorinated sample initially selected was partially measured after sixteen days of exposure to air. Some results for this sample are shown, but were not analyzed in detail since a complete set of data could not be obtained.

Resistivity, magnetoresistance, and Hall-effect measurements were carried out with a PPMS$^{@}$ manufactured by Quantum Design Inc. Temperatures were varied in the range 2 K – 250 K, and magnetic fields up to 9 T were applied. A probe current of 100 nA was used in most experiments since this value is safely inside the linear range in the I–V characteristics.

Fig. 1 shows the sheet resistance, R_S, of the studied samples as a function of temperature. It was determined as $R_S = R(W/L)$, where R is the measured resistance, L is the distance between the electrodes used to measure voltage, and W is the film width [13]. The length L is the largest source for absolute uncertainty in the determination of R_S. This systematic source of error amounts to at most 5% of the reported R_S values. Uncertainties due to electronic instabilities are smaller than the size of the experimental points.

Results in Fig. 1 shows that chlorination causes a significant overall reduction of R_S. As mentioned before, Cl adsorption on graphene should produce p-type doping, and the strong decrease of R_S upon chlorination is consistent with this scenario. At $T = 200$ K, the sheet resistance of the pristine sample CVDg is approximately three times larger than that of the chlorinated CVDg-Cl(1 day) measured 1 day after the Cl incorporation. Also interesting to note in Fig. 1 is the time stability of R_S in the chlorinated samples within short periods. The measurement performed nine days past chlorination, [sample CVDg-Cl(9 days)] nearly reproduces that for CVDg-Cl(1 day), although no special care was taken to store the sample during the intervening time. However, data for CVDg-Cl(16 days) suggests that the Cl content decreases substantially in periods above two weeks. The resistivity for this sample lies in between that for the pristine sample and those of samples annealed for shorter periods.

The overall resistive behavior observed for CVDg is consistent with previously reported measurements [14,15]. The low-temperature upturn of sheet resistances shown in Fig. 1 indicates the occurrence of electron-localization effects [14,16]. Heo et al. [14], reporting on the temperature-dependent resistivity of CVD-graphene samples showing a crossover from metallic- to insulator-like behavior at low temperature, proposed an explanation based on the interplay between electron–phonon scattering and thermally activated transport in an inhomogeneous medium. The inhomogeneities were pictured as carrier puddles due to electric field fluctuations caused by random charged impurities or other defects, either incorporated in the graphene or existing in the underlying environment (mostly the substrate). Alternatively, a temperature-dependent resistivity consistent with a hopping-type mechanism was suggested in the case of a hydrogenated sample obtained from exfoliated graphene [17]. Thus, a superposition of scattering mechanisms might be involved in the resistivity behavior, mainly in the low-temperature limit. The upturn of sheet resistances in Fig. 1 is quantitatively significant. It cannot be described solely based on weak quantum perturbations to the otherwise dominant Boltzmann-type transport. Nevertheless, important complementary information

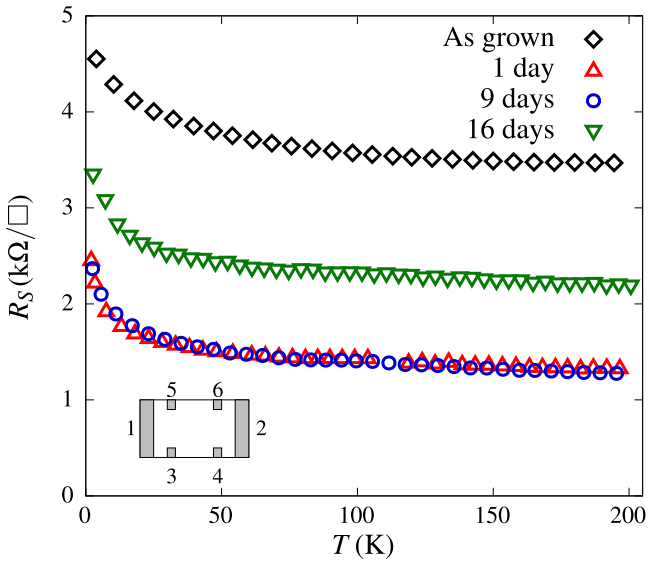

Fig. 1. Sheet resistance as a function of temperature for the studied CVD-graphene samples. The indicated number of days refers to the time between preparation and measurement for the Cl-doped samples. The inset shows a schematic representation of the contact geometry and wiring. Current was applied between contacts 1 and 2, longitudinal voltage measured between contacts 3 and 4 (to evaluate resistance), and transverse voltage (for Hall effect) between contacts 3 and 5. The largest source for systematic uncertainties in the sheet resistance measurements comes from the distance between contacts and amounts to 5% at most of the reported values.

may be obtained from magnetoresistance measurements. In this context, the weak-localization (WL) theory [18,19] was proposed as the appropriate interpretation framework [20–24], although in some cases the WL seems to be strongly suppressed or even absent [25].

Fig. 2 shows the magnetoresistance (MR) results for the three investigated samples. The experiments were carried out in several fixed temperatures, ranging from 2 K to 200 K, and applied fields up to $\mu_0 H = 9$ T. The observed noise comes mostly from fluctuations in the impedance of the electrical contacts. Contrasting with results for clean graphene [26], Shubnikov–de Haas oscillations are not visible in our samples due to structural disorder and the relatively low intensity of the applied magnetic fields. On the other hand, weak-localization and weak-antilocalization (WAL) contributions are observed in the MR at low temperatures for the pristine CVDg sample shown in Fig. 2(a) and for CVDg-Cl(9 days), as shown in Fig. 2(c).

The interplay between WL and WAL is also seen in the MR results for CVDg-Cl(16 days) at $T = 2$ K, as depicted in the inset of Fig. 2(c). The negative magnetoresistance at low applied fields is a signature of WL, whereas a positive contribution at intermediate and high fields can be attributed to WAL. The results for CVDg-Cl(1 day) are shown in Fig. 2(b). In this case, the WL contribution is clearly dominant at low temperatures. However, above 20 K two-band conduction must be taken into account, mostly for the pure CVDg and the CVDg-Cl(9 days) samples. Even though it is possible that defects occurring in CVD graphene modify its electronic structure, opening a small gap near the Fermi level [27], at high enough temperatures both valence and conduction bands play important roles in the charge-transport properties of this material. Above $T = 20$ K the magnetoresistance of the CVDg and CVDg-Cl(9 days) samples is clearly dominated by a positive B^2 field dependence, as expected from the Lorentz-force effect in two-band conductors [28]. The role of two-carrier transport as well as its interplay with weak and strong localization effects in several graphene devices were previously addressed by Hilke et al. [24]. It is interesting to note in Fig. 2 that at high temperatures the magnetoresistance of the CVDg-Cl(1 day) and CVD-Cl(9 days) samples increases approximately linearly with the applied field. This behavior has been observed in systems with

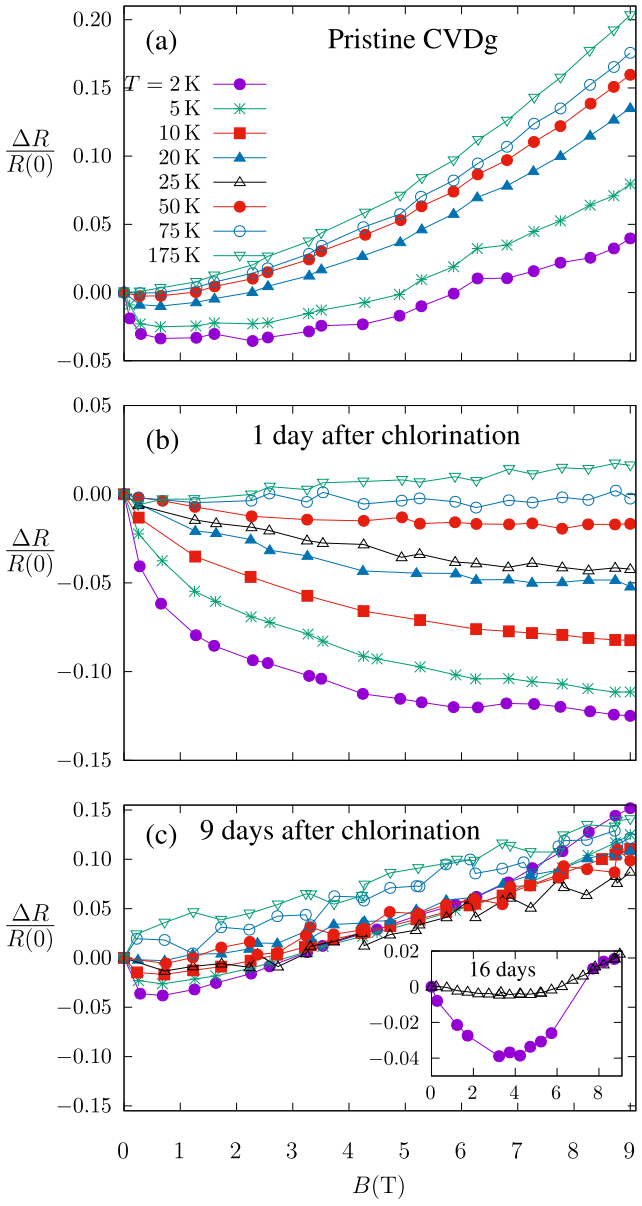

Fig. 2. Measured relative magnetoresistance as a function of magnetic field at several temperatures for (a) the pristine CVDg sample, (b) the freshly doped CVDg-Cl(1 day) sample, and (c) the aged CVDg-Cl(9 days) sample. The inset in panel (c) shows results at $T = 2$ K and $T = 25$ K for the CVDg-Cl(16 days) sample.

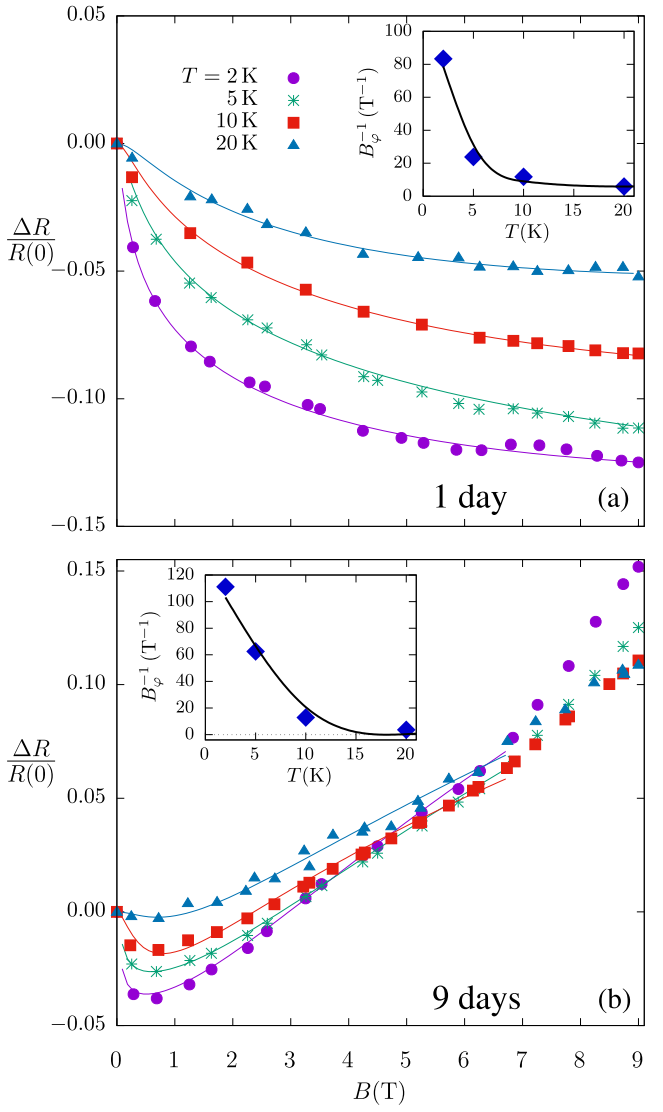

Fig. 3. Fitting of Eq. (1) to the experimental MR results at low temperatures for the samples (a) CVDg-Cl(1 day) and (b) CVDg-Cl (9 days). The behavior of B_φ^{-1} (insets) reflects the loss of coherence (reduction of τ_φ) with increasing temperature.

small Fermi surfaces. Spatial mobility fluctuations related to disorder were proposed as a possible origin for this phenomenon [29].

According to the WL theory [19], two scattering rates should be taken into account: $1/\tau_\varphi$, related to the phase-coherence time, and $1/\tau_e$, the elastic scattering rate. Weak-localization effects are originated from enhanced back-scattering, implying that $\tau_\varphi \gg \tau_e$, so that a charge carrier may suffer several elastic collisions before losing phase coherence.

Starting with a seminal work by McCann et al. [20], detailed theoretical and experimental approaches to describe WL effects in graphene have been developed [21,24], in which two types of elastic scattering rates are considered. One is related to carrier scattering between K and K′ points of the Brillouin zone (intervalley scattering), with characteristic time denoted as τ_i, while the other is associated to scattering processes occurring within a valley, with relaxation time τ_*. It was theoretically demonstrated that WL effects are relevant in graphene samples in which intervalley scattering is prominent. From Refs. [20,21,24], the relative magnetoresistance in single-layer graphene may be written as

$$\frac{\Delta R}{R(0)} = -\frac{e^2 R(0)}{\pi h}\left[F\left(\frac{B}{B_\varphi}\right) - F\left(\frac{B}{B_\varphi + 2B_i}\right) - 2F\left(\frac{B}{B_\varphi + B_i + B_*}\right)\right], \tag{1}$$

where $R(0)$ is the resistance at zero magnetic field, e is the electron charge, h is Planck's constant, and the dependence on the applied induction B occurs through the function $F(z) = \ln z + \psi(\frac{1}{2} + \frac{1}{z})$, where ψ is the digamma function. The characteristic inductions appearing in the arguments of $F(z)$ are related to the relaxation times as $B_\nu = \hbar c/4De\tau_\nu$, where $\nu = (\varphi, i, *)$ and D is the diffusion constant. This is valid in a regime of long-time coherence, which implies that $B_\varphi \ll B_*$.

In Fig. 3 we show fittings of Eq. (1) to the low-temperature MR measurements for the CVDg-Cl(1 day) and CVD-Cl(9 days) samples. For the freshly Cl-doped sample, shown in panel (a) of Fig. 3, a good fit could be obtained for temperatures up to $T = 20$ K in the whole range of applied fields. The values obtained for the fitting parameters are listed in Table 1.

Table 1
Values of the magnetic-field parameters associated to the relevant scattering rates for different temperatures, obtained by fitting Eq. (1) to our magnetoresistance data for the indicated samples. The percentual uncertainties for the adjusted parameters are in parentheses.

Sample	T(K)	B_φ(T)	B_i(T)	B_*(T)
CVDg	2	1.8×10^{-2} (2%)	6.5×10^{-4} (2%)	6.3 (1%)
	5	2.3×10^{-2} (3%)	1.9×10^{-4} (3%)	10.5 (2%)
CVDg-Cl(1 day)	2	1.2×10^{-2} (2%)	2.1 (7%)	2.4 (13%)
	5	4.6×10^{-2} (2%)	4.1 (25%)	5.7 (38%)
	10	8.5×10^{-2} (2%)	2.9 (10%)	2.9 (21%)
	20	1.7×10^{-1} (8%)	1.6 (5%)	1.8 (9%)
CVDg-Cl(9 days)	2	0.9×10^{-2} (21%)	1.9×10^{-3} (31%)	1.1 (8%)
	5	1.6×10^{-2} (16%)	2.8×10^{-3} (27%)	1.2 (8%)
	10	1.6×10^{-2} (18%)	1.8×10^{-3} (28%)	1.3 (7%)
	20	3.2×10^{-2} (22%)	6.0×10^{-4} (18%)	1.5 (11%)

In all cases, intravalley scattering is dominant, with $B_* \sim 1$ T, while B_φ is smaller by two orders of magnitude. Although B_φ grows with temperature (see insets of Fig. 3), reflecting the expected loss of phase coherence due to inelastic scattering events, it remains smaller than B_* by one order of magnitude. It is worth mentioning that the B_φ magnitudes that we found at low temperatures ($T \simeq 5$ K) correspond to pair-breaking lengths $L_\varphi = \sqrt{\hbar/eB_\varphi} \simeq 115$ nm for CVDg-Cl(1 day), and $L_\varphi \simeq 200$ nm for CVDg(9 days). These values are well within the range of parameters reported by Hong et al. [30], obtained from magnetoresistance measurements in fluorine-doped exfoliated graphene. On the other hand, $L_\varphi = 300 - 700$ nm was found in a tungsten-decorated exfoliated-graphene device [31], suggesting that perturbation in the graphene plane is significantly smaller in this case than with halogens as the adsorbed atoms.

Our fittings in Fig. 3 reveal that the main difference in the magnetoresistance behavior with the applied field between the two samples is due to the strength of intervalley scattering. One day after chlorination we obtain a $B_i \sim B_*$, but B_i is reduced by at least three orders of magnitude when measured after nine days. The effect of these changes in scattering rates on the magnetoresistance can be understood by inspecting Eq. (1). The function $F(z)$ is a positive-definite, monotonically growing function of its argument. Thus, if $B_i \ll B_\varphi$ the first two terms on the right-hand side of Eq. (1) tend to cancel out, and the positive contribution of the intravalley-scattering term dominates at a sufficiently large applied field. The latter can be identified as a WAL effect. On the other hand, if $B_i \sim B_* \gg B_\varphi$ the phase-coherence term is dominant, and the MR remains negative with increasing field. For the aged CVDg-Cl(9 days) sample, the positive deviations of the measured MR with respect to the theoretical expectation at high fields, as well as the crossing of fitting lines occurring between 4 and 7 teslas, are likely due to an additional B^2 normal magnetoresistance contribution which becomes dominant at temperatures higher than 20 K, as seen in Fig. 2(c).

From the above discussion, it is clear that the negative MR due to WL in graphene has its origin in the occurrence of significant intervalley scattering. This is mainly observed in our CVDg-Cl(1 day) sample, whose distinctive feature is its strong doping. Besides increasing carrier density, one may infer that adsorbed Cl atoms generate localized lattice distortions, providing scattering centers that allow for large momentum transfer. Indeed, it is known that chlorination causes a graphene layer to corrugate in order to accommodate the Cl atoms [10]. Besides, one may suppose that the incorporated halogen atoms themselves act as scattering centers. Such a possibility was proposed in Ref. [30], where it is suggested that F adatoms introduce local moments, leading to spin-dependent scattering.

Magnetoresistance results for the pristine CVDg sample are strongly affected by the Lorentz term, as may be inferred from a mere visual inspection of Fig. 2(a). There, one sees that the MR becomes entirely positive and weakly dependent on temperature for $T \gtrsim 50$ K, as expected for a magnetoresistance driven by the Lorentz force. Nevertheless, for $T = 2$ K and $T = 5$ K, fittings of Eq. (1) to the experimental MR curves lead to parameter values similar to those obtained for the aged Cl-doped sample. This shows that WL and WAL effects are also relevant for describing the magnetotransport properties of our undoped CVD graphene sample.

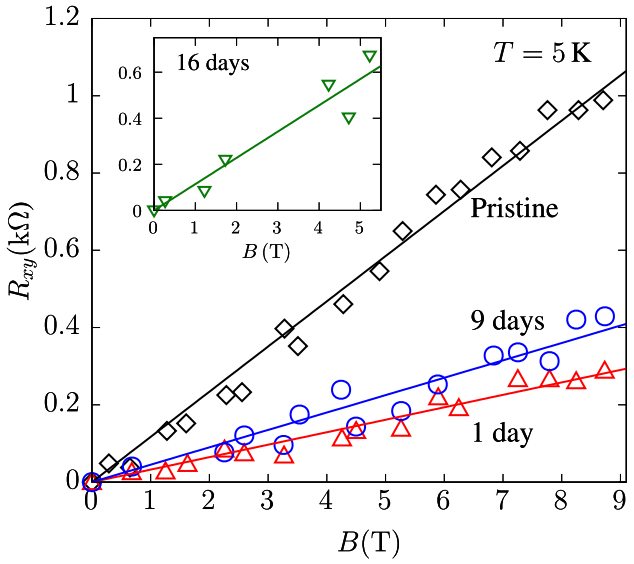

Fig. 4. Hall resistance as a function of the applied field at $T = 5$ K for the three studied CVD-graphene samples. The inset shows partial results for sample CVDg-Cl(16 days).

In Fig. 4, representative Hall-resistance data obtained at $T = 5$ K are shown as a function of the applied field for the three investigated samples. Similar results were obtained at temperatures up to 10 K. Reliable results for the CVDg-Cl (16 days), shown in the inset of Fig. 4, were restricted to the field range $B \lesssim 5$ T. For temperatures above 20 K, Hall measurements in all samples become too noisy, so that trustful results could not be obtained. This fact suggests that a significant reduction of the Hall constant in our graphene samples occur in the intermediate- to the high-temperature range. This is expected if two nearly-compensated carrier bands contribute to electrical transport, as also suggested by the magnetoresistance experiments.

The Hall resistance is defined as $R_{xy} = V_{xy}/I_{xx}$, where V_{xy} is the measured transverse voltage and I_{xx} the applied longitudinal current. The Lorentz-force contribution to Hall resistance is given by $R_{xy} = R_0 B$, where $R_0 = 1/p_s e$ is the ordinary Hall coefficient, p_s being the surface carrier density. To derive the Hall coefficient and estimate the carrier density, straight lines are fitted through the data points in Fig. 4. The same was done for measurements carried out at $T = 2$ K and $T = 10$ K, except for the sample annealed for 16 days, in which case only the experiment at $T = 5$ K could be done. Hall coefficients obtained from these experiments do not vary with temperature.

The fact that R_0 is positive for all the studied samples indicates that the dominant charge carriers are holes in all cases. The resulting values of p_s for the studied samples are listed in Table 2. These values are averages calculated from measurements performed at $T = 2$ K, 5 K, and 10 K. The values of p_s in Table 2 are in reasonable agreement with those obtained from Hall measurements using the van der Pauw method in similar pure and chlorinated CVD graphene samples [10]. We also note that the ratio between p_s values for each chlorinated sample and the pristine one is close to that estimated from simply comparing the resistances displayed in Fig. 1. Mobilities at $T = 250$ K, determined as $\mu = (e\, p_s R_S)^{-1}$, are also listed in Table 2.

The values for μ in our samples fall in the range of commonly reported values for CVD-grown graphene [6]. It is worth remarking that values of p_s and μ reported for the CVDg-Cl(16 days) sample in Table 2

Table 2
Hole-type carrier density (p_s) and mobility (μ) estimated from Hall-effect measurements carried out at low temperatures in the listed CVD-graphene samples. The percentual uncertainties for the estimated quantities are indicated in parentheses.

Sample	p_s (10^{12} cm^{-2})	μ (cm^2/Vs)
CVDg	5.3 (9%)	347 (8%)
CVDg-Cl(1 day)	19.4 (7%)	269 (7%)
CVDg-Cl(9 days)	13.9 (9%)	374 (8%)
CVDg-Cl(16 days)	5.5 (22%)	430 (18%)

are to be taken as indicative. Errors are large in this case. One observes that the mobility shows a marked decrease when chlorine adatoms are freshly incorporated into CVD graphene. Then a tendency occurs to recover and surpass the value characterizing the pristine sample as the chlorine is progressively desorbed from the sample. Probably, the corrugation in the graphene plane caused by the Cl adsorption [10] increases the carrier scattering rate, thus producing the decrease of μ in the functionalized samples.

The results in Table 2 confirm that room-temperature annealing during nine and sixteen days led to Cl loss, as revealed by the observed decrease in the estimated hole density. According to Fig. 1, however, the CVDg-Cl(1 day) and CVDg-Cl(9 days) samples have practically the same resistances. We interpret this fact as a consequence of a reduced disorder in the annealed sample, which is also due to the loss of Cl atoms by their role as scattering centers. Since the resistivity depends on the product $p_s\tau$, a small decrease of p_s in the annealed sample is compensated by an increase in the relaxation time, so that the resistivity remains approximately invariant. We also observed that further aging of the samples consistently leads to an increase in resistivity, as the loss of carriers due to dechlorination becomes the dominant effect. For instance, for the sample aged 16 days we obtain a 70% higher R_S in comparison to the CVDg-Cl(9 days) sample, as shown in Fig. 1. The scenario of a reduced disorder characterizing the CVDg-Cl(9 days) sample is also consistent with the magnetoresistance analysis in Fig. 3. Comparison of the fitted parameter values (Table 1) reveals a slight reduction of B_* and a very strong decrease of B_i with respect to the values obtained one day after chlorination.

Earlier works [32,33] report the occurrence of a substantial enhancement of the conductivity and Hall mobility in single and multilayer chlorinated graphene samples when compared to pristine graphene. We also mention that the quantum Hall effect was observed in exfoliated single-layer samples at high applied fields [34], and a spin-Hall effect [35] has been reported to occur in CVD graphene deposited on copper. Our work, however, focused on the ordinary Hall effect, aiming to examine the carrier density in order to provide complementary information to transport measurements.

3. Conclusions

We presented results of magnetotransport experiments carried out in single-layer graphene grown by chemical vapor deposition. Samples were submitted to a photochlorination process, and a pristine sample was also investigated for comparison. Resistivity and Hall-effect measurements showed that a significant hole doping was achieved in the functionalized samples. The Hall-effect experiments also revealed that a moderate Cl desorption occurs when submitting chlorinated samples to room-temperature annealing for a few days, although desorption seems to be significant for periods above two weeks.

The magnetoresistance experiments performed at low temperatures unequivocally revealed weak-localization effects. A negative MR characteristic of weak localization was shown to be the dominant contribution in a freshly Cl-doped sample, which presents the highest carrier density as determined by the ordinary Hall coefficient. After annealing this sample at room temperature for nine days, the MR at low temperatures was substantially modified, with an upturn occurring in the low-field region. We interpret this behavior as resulting from an interplay between weak localization and weak antilocalization theoretically predicted to occur in graphene when intervalley scattering is relevant [20]. The competition between these two effects leads to a sign reversal in the MR, which is negative at low magnetic fields but eventually becomes positive when the field is continuously increased. The MR of the non-doped sample also shows WL and WAL contributions.

A theoretical expression for the magnetoresistance in the presence of weak-localization [20,24] was successfully fitted to our experimental results at low temperatures, confirming the role of intervalley scattering as responsible for weak-localization effects in graphene. Our results extend to a considerably higher field range former observations of the weak-localization properties in graphene flakes [21–24], allowing full verification of the theoretical predictions [20,24]. Using CVD grown samples functionalized with chlorine, hole doping was varied by simply aging the samples at room temperature. At intermediate and high temperatures the MR for all studied samples becomes positive and roughly proportional to B^2, which is consistent with the occurrence of two-band conduction.

Our electrical transport experiments in graphene grown by CVD confirms that functionalization with Cl adatoms produces a substantial hole doping. This leads to a strong decrease in the resistivity of freshly chlorinated samples. On the other hand, chlorination enhances effects from disorder in the transport properties. These findings should be considered when practical applications of this material are envisaged.

CRediT authorship contribution statement

F. Mesquita: Experiments, Preparation of figures, Typing of the text. **G. Copetti:** Samples' preparation. **M.A. Tumelero:** Experiments, Handling of equipments. **M.A. Gusmão:** Theoretical analysis, Writing - original draft. **C. Radtke:** Samples' preparation, Writing - original draft. **P. Pureur:** General coordination, Conception of the work, Writing - original draft, Submission.

Declaration of competing interest

The authors declare that they have no known competing financial interests or personal relationships that could have appeared to influence the work reported in this paper.

Acknowledgments

This research was supported by Conselho Nacional de Desenvolvimento Científico e Tecnológico (CNPq), Brazil and Fundação de Amparo à Pesquisa do Estado do Rio Grande do Sul (FAPERGS), Brazil, under the joint program PRONEX, grant no. 16/0490-0. F.M. benefits from a post-doctoral fellowship of Coordenação de Aperfeiçoamento de Pessoal de Nível Superior (CAPES), Brazil.

References

[1] A.K. Geim, Graphene: Status and prospects, Science 324 (5934) (2009) 1530–1534, http://dx.doi.org/10.1126/science.1158877, URL https://science.sciencemag.org/content/324/5934/1530.
[2] E.L. Wolf, Applications of Graphene: An Overview, Springer, Cham, 2014, http://dx.doi.org/10.1007/978-3-319-03946-6.
[3] A.H. Castr Neto, F. Guinea, N.M.R. Peres, K.S. Novoselov, A.K. Geim, The electronic properties of graphene, Rev. Modern Phys. 81 (2009) 109–162, http://dx.doi.org/10.1103/RevModPhys.81.109, URL https://link.aps.org/doi/10.1103/RevModPhys.81.109.
[4] Y. Cao, V. Fatemi, S. Fang, K. Watanabe, T. Tanigushi, E. Kaxiras, P. Jarrilo-Herrero, Unconventional superconductivity in magic-angle graphene superlattices, Nature 556 (2018) 43–50, http://dx.doi.org/10.1038/nature26160.
[5] R. Muñoz, C. Gomez-Aleixandre, Review of CVD synthesis of graphene, Chem. Vapor Depos. 19 (2013) 297–322, http://dx.doi.org/10.1002/cvde.201300051, URL https://onlinelibrary.wiley.com/doi/abs/10.1002/cvde.201300051.
[6] D. Wei, Y. Liu, Y. Wang, H. Zhang, L. Huang, G. Yu, Synthesis of N-doped graphene by chemical vapor deposition and its electrical properties, Nano Lett. 9 (5) (2009) 1752–1758, http://dx.doi.org/10.1021/nl803279t, pMID: 19326921.

[7] Y.-F. Lu, S.-T. Lo, J.-C. Lin, W. Zhang, J.-Y. Lu, F.-H. Liu, C.-M. Tseng, Y.-H. Lee, C.-T. Liang, L.-J. Li, Nitrogen-doped graphene sheets grown by chemical vapor deposition: Synthesis and influence of nitrogen impurities on carrier transport, ACS Nano 7 (8) (2013) 6522–6532, http://dx.doi.org/10.1021/nn402102y, pMID: 23879622.

[8] W. Wei, X. Qu, Extraordinary physical properties of functionalized graphene, Small 8 (14) (2012) 2138–2151, http://dx.doi.org/10.1002/smll.201200104, URL https://pubmed.ncbi.nlm.nih.gov/22674906.

[9] V.P. Pham, K.N. Kim, M.H. Jeon, K.S. Kim, G.Y. Yeom, Cyclic chlorine trap-doping for transparent, conductive, thermally stable and damage-free graphene, Nanoscale 6 (2014) 15301–15308, http://dx.doi.org/10.1039/C4NR04387A.

[10] G. Copetti, E.H. Nunes, G.K. Rolim, G.V. Soares, S.A. Correa, D.E. Weibel, C. Radtke, Reversibility of graphene photochlorination, J. Phys. Chem. C 122 (28) (2018) 16333–16338, http://dx.doi.org/10.1021/acs.jpcc.8b02121.

[11] B. Li, L. Zhou, D. Wu, H. Peng, K. Yan, Y. Zhou, Z. Liu, Photochemical chlorination of graphene, ACS Nano 5 (7) (2011) 5957–5961, http://dx.doi.org/10.1021/nn201731t, pMID: 21657242.

[12] C.M. Hurd, The Hall Effect in Metals and Alloys, Springer, Boston, 1992, http://dx.doi.org/10.1007/978-1-4757-0465-5.

[13] S. De, J.N. Coleman, Are there fundamental limitations on the sheet resistance and transmittance of thin graphene films? ACS Nano 4 (5) (2010) 2713–2720, http://dx.doi.org/10.1021/nn100343f, pMID: 20384321.

[14] J. Heo, H.J. Chung, S.-H. Lee, H. Yang, D.H. Seo, J.K. Shin, U.-I. Chung, S. Seo, E.H. Hwang, S. Da. Sarma, Nonmonotonic temperature dependent transport in graphene grown by chemical vapor deposition, Phys. Rev. B 84 (2011) 035421, http://dx.doi.org/10.1103/PhysRevB.84.035421, URL https://link.aps.org/doi/10.1103/PhysRevB.84.035421.

[15] A.V. Babichev, V.E. Gasumyants, V.Y. Butko, Resistivity and thermopower of graphene made by chemical vapor deposition technique, J. Appl. Phys. 113 (7) (2013) 076101, http://dx.doi.org/10.1063/1.4792032.

[16] J.-H. Chen, W.G. Cullen, C. Jang, M.S. Fuhrer, E.D. Williams, Defect scattering in graphene, Phys. Rev. Lett. 102 (2009) 236805, http://dx.doi.org/10.1103/PhysRevLett.102.236805, URL https://link.aps.org/doi/10.1103/PhysRevLett.102.236805.

[17] C. Chuang, R. Puddy, H.-D. Lin, S.-T. Lo, T.-M. Chen, C. Smith, C.-T. Liang, Experimental evidence for efros–shklovskii variable range hopping in hydrogenated graphene, Solid State Commun. 152 (10) (2012) 905–908, http://dx.doi.org/10.1016/j.ssc.2012.02.002, URL http://www.sciencedirect.com/science/article/pii/S0038109812000853.

[18] B.L. Altshuler, D. Khmel'nitzkii, A.I. Larkin, P.A. Lee, Magnetoresistance and hall effect in a disordered two-dimensional electron gas, Phys. Rev. B 22 (1980) 5142–5153, http://dx.doi.org/10.1103/PhysRevB.22.5142, URL https://link.aps.org/doi/10.1103/PhysRevB.22.5142.

[19] G. Bergmann, Weak localization in thin films: a time-of-flight experiment with conduction electrons, Phys. Rep. 107 (1) (1984) 1–58, http://dx.doi.org/10.1016/0370-1573(84)90103-0, URL http://www.sciencedirect.com/science/article/pii/0370157384901030.

[20] E. McCann, K. Kechedzhi, V.I. Fal'ko, H. Suzuura, T. Ando, B.L. Altshuler, Weak-localization magnetoresistance and valley symmetry in graphene, Phys. Rev. Lett. 97 (2006) 146805, http://dx.doi.org/10.1103/PhysRevLett.97.146805, URL https://link.aps.org/doi/10.1103/PhysRevLett.97.146805.

[21] D. Horsell, F. Tikhonenko, R. Gorbachev, A. Savchenko, Weak localization in monolayer and bilayer graphene, Phil. Trans. R. Soc. A 366 (1863) (2008) 245–250, http://dx.doi.org/10.1098/rsta.2007.2159, URL https://royalsocietypublishing.org/doi/abs/10.1098/rsta.2007.2159.

[22] F.V. Tikhonenko, D.W. Horsell, R.V. Gorbachev, A.K. Savchenko, Weak localization in graphene flakes, Phys. Rev. Lett. 100 (2008) 056802, http://dx.doi.org/10.1103/PhysRevLett.100.056802, URL https://link.aps.org/doi/10.1103/PhysRevLett.100.056802.

[23] F.V. Tikhonenko, A.A. Kozikov, A.K. Savchenko, R.V. Gorbachev, Transition between electron localization and antilocalization in graphene, Phys. Rev. Lett. 103 (2009) 226801, http://dx.doi.org/10.1103/PhysRevLett.103.226801, URL https://link.aps.org/doi/10.1103/PhysRevLett.103.226801.

[24] M. Hilke, M. Massicotte, V.Y. Eri. Whiteway, Weak localization in graphene: Theory, simulations, and experiments, Sci. World J. 2014 (737296) (2014) 8, http://dx.doi.org/10.1155/2014/737296.

[25] S.V. Morozov, K.S. Novoselov, M.I. Katsnelson, F. Schedin, L.A. Ponomarenko, D. Jiang, A.K. Geim, Strong suppression of weak localization in graphene, Phys. Rev. Lett. 97 (2006) 016801, http://dx.doi.org/10.1103/PhysRevLett.97.016801, URL https://link.aps.org/doi/10.1103/PhysRevLett.97.016801.

[26] Z. Tan, C. Tan, L. Ma, G.T. Liu, L. Lu, C.L. Yang, Shubnikov-de haas oscillations of a single layer graphene under dc current bias, Phys. Rev. B 84 (2011) 115429, http://dx.doi.org/10.1103/PhysRevB.84.115429, URL https://link.aps.org/doi/10.1103/PhysRevB.84.115429.

[27] D. Wei, Y. Liu, Y. Wang, H. Zhang, L. Huang, G. Yu, Synthesis of N-doped graphene by chemical vapor deposition and its electrical properties, Nano Lett. 9 (5) (2009) 1752–1758, http://dx.doi.org/10.1021/nl803279t, pMID: 19326921.

[28] J.M. Ziman, Principles of the Theory of Solids, second ed., Cambridge University Press, Cambridge, 1972, http://dx.doi.org/10.1017/CBO9781139644075.

[29] A. Narayanan, M.D. Watson, S.F. Blake, N. Bruyant, L. Drigo, Y.L. Chen, D. Prabhakaran, B. Yan, C. Felser, T. Kong, P.C. Canfield, A.I. Coldea, Linear magnetoresistance caused by mobility fluctuations in n-doped Cd_3As_2, Phys. Rev. Lett. 114 (2015) 117201, http://dx.doi.org/10.1103/PhysRevLett.114.117201, URL https://link.aps.org/doi/10.1103/PhysRevLett.114.117201.

[30] X. Hong, K. Zou, B. Wang, S.-H. Cheng, J. Zhu, Evidence for spin-flip scattering and local moments in dilute fluorinated graphene, Phys. Rev. Lett. 108 (2012) 226602, http://dx.doi.org/10.1103/PhysRevLett.108.226602, URL https://link.aps.org/doi/10.1103/PhysRevLett.108.226602.

[31] J.A. Elias, E.A. Henriksen, Electronic transport and scattering times in tungsten-decorated graphene, Phys. Rev. B 95 (2017) 075405, http://dx.doi.org/10.1103/PhysRevB.95.075405, URL https://link.aps.org/doi/10.1103/PhysRevB.95.075405.

[32] X. Zhang, A. Hsu, H. Wang, Y. Song, J. Kong, M.S. Dresselhaus, T. Palacios, Impact of chlorine functionalization on high-mobility chemical vapor deposition grown graphene, ACS Nano 7 (8) (2013) 7262–7270, http://dx.doi.org/10.1021/nn4026756, pMID: 23844715.

[33] V.P. Pham, A. Mishra, G. Youn Yeom, The enhancement of hall mobility and conductivity of CVD graphene through radical doping and vacuum annealing, RSC Adv. 7 (2017) 16104–16108, http://dx.doi.org/10.1039/C7RA01330B.

[34] K.S. Novoselov, Z. Jiang, Y. Zhang, S.V. Morozov, H.L. Stormer, U. Zeitler, J.C. Maan, G.S. Boebinger, P. Kim, A.K. Geim, Room-temperature quantum hall effect in graphene, Science 315 (5817) (2007) 1379, http://dx.doi.org/10.1126/science.1137201, URL https://science.sciencemag.org/content/315/5817/1379.

[35] J. Balakrishnan, G.K.W. Koon, A. Avsar, Y. Ho, J.H. Lee, M. Jaiswal, S.-J. Baeck, J.-H. Ahn, A. Ferreira, M.A. Cazalilla, A.H.C. Neto, B. Ozyilmaz, Giant spin hall effect in graphene grown by chemical vapour deposition, Nature Commun. 5 (5748) (2014) 1–5, http://dx.doi.org/10.1038/ncomms5748.